Surface Science xxx (2015) xxx–xxx

Contents lists available at ScienceDirect

Surface Science

journal homepage: www.elsevier.com/locate/susc

The influence of CO adsorption on the surface composition of cobalt/palladium alloys

A. Murdoch [a], A.G. Trant [b], J. Gustafson [a,1], T.E. Jones [a], T.C.Q. Noakes [b], P. Bailey [b], C.J. Baddeley [a,*]

[a] EaStCHEM School of Chemistry, University of St Andrews, St Andrews, Fife, KY16 9ST, UK
[b] UK MEIS Facility, STFC Daresbury Laboratory, Warrington, Cheshire, WA4 4AD, UK

ARTICLE INFO

Available online xxxx

Keywords:
Medium energy ion scattering
Vibrational spectroscopy
Alloy

ABSTRACT

Segregation induced by the adsorption of gas phase species can strongly influence the composition of bimetallic surfaces and can therefore play an important role in influencing heterogeneous catalytic reactions. The addition of palladium to cobalt catalysts has been shown to promote Fischer Tropsch catalysis. We investigate the adsorption of CO onto bimetallic CoPd surfaces on Pd{111} using a combination of reflection absorption infrared spectroscopy and medium energy ion scattering. The vibrational frequency of adsorbed CO provides crucial information on the adsorption sites adopted by CO and medium energy ion scattering probes the surface composition before and after CO exposure. We show that cobalt segregation is induced by CO adsorption and rationalise these observations in terms of the strength of adsorption of CO in various surface adsorption sites.

Introduction

Since the 1920s, the Fischer–Tropsch reaction [1] has been an industrially important method of converting of synthesis gas ($CO + H_2$) derived from coal, natural gas, oil, biomass, etc., into longer chain hydrocarbons (e.g. components of gasoline) and other high-value organic chemicals. Much of the research into these processes has utilised Fe- or Co-based catalysts.[2–4] The doping of Co catalysts with metals such as Pd has resulted in improved performance in the conversion of methane to hydrocarbons [5] and CO hydrogenation.[6] A number of catalytic investigations [5–7] and model studies on CoPd nanoparticles grown on a flat alumina film [8–11] have investigated the promoting effect of Pd and it is proposed that the role of Pd is to enhance the adsorption of H_2 to facilitate the reduction of cobalt oxide forming the more active metallic phase.

There are many examples of bimetallic catalysts in industrial use [12–14]. The promoting effect of adding a second element is often ascribed to effects related to surface structure (ensemble effects) or surface electronic properties (ligand effects). As elegantly described by Liu and Nørskov [15], these effects can be explained in a quantitative manner by the following example. An isolated Pd atom in a {111} surface surrounded by six Au atoms adsorbs CO in an on-top geometry with a binding energy of ~0.7 eV [15]. The adsorption of CO in a hollow site surrounded by three Pd atoms has a binding energy of ~1.1 eV [15]. Thus the availability of Pd_3 clusters surrounding three-fold hollow sites has a dramatic effect on the adsorption of CO. This is an example of an ensemble effect. Ligand effects are electronic in origin and may be ascribed to charge transfer from one element to another [16]. The relative magnitude of these phenomena dictates which effect dominates in the catalytic process.

An additional effect, often ignored in explaining catalytic behaviour, is the influence of the gas phase on the composition of a bimetallic surface. It is well known that the surface composition of a bimetallic particle will differ from the bulk composition due to a number of inter-related effects such as the relative atomic size, the relative surface energies, and the exposed crystal faces. When a bimetallic surface is exposed to a reactive gas phase, assuming that any diffusion barriers are surmountable, the surface composition of the bimetallic surface is modified in order to produce the most favourable interaction with the adsorbed species. In many cases, the element which interacts most strongly with the adsorbate segregates to the surface [17], but there are often more subtle effects. For example, Pt interacts much more strongly with CO than Cu, but Chorkendorff and co-workers showed that CO-induced Cu segregation to the {111} surface of a CuPt alloy [18]. The driving force in this case was concluded to be the very favourable adsorption of CO on single Pt atoms surrounded by 6 Cu atoms. Recently, Rupprechter and co-workers investigated the adsorption of CO on a PdZn {111} surface and demonstrated that the atoms in the surface plane can rearrange to maximise the interaction with the adsorbed species [19].

In this study, we used reflection absorption infrared spectroscopy (RAIRS) and medium energy ion scattering (MEIS) to probe the effect of CO adsorption on the surface composition of bimetallic CoPd surfaces as a function of initial Pd composition. We recently reported a MEIS study of the growth and alloying behaviour of Co thin films on

* Corresponding author. Tel.: +44 1334 467236; fax: +44 1334 463808.
E-mail address: cjb14@st-and.ac.uk (C.J. Baddeley).
[1] Present address: Div. of Synchrotron Radiation Research, Lund University, Box 118, 221 00 Lund, Sweden.

http://dx.doi.org/10.1016/j.susc.2015.08.004
0039-6028/

Pd{111} at 300 K [20]. Growth at 300 K was found to occur via the Volmer–Weber growth mode. MEIS analysis of a ~6 ML Co film on Pd{111} showed that initial growth occurred either in an fcc mode with a subsequent switch to hcp growth or via the simultaneous nucleation of crystallites of each structure type with an approximately equal probability. Annealing to 400–450 K caused the surface to flatten with no surface Pd visible in MEIS spectra. Annealing the Co film to higher temperatures caused interdiffusion and produced two temperature regions of compositional stability. Between 550 and 650 K, LEED, STM, and MEIS are consistent with the formation of three rotationally equivalent p(2 × 1) phases consisting of the {111} termination of the bulk ordered CoPd alloy ($L1_o$ CuAu structure). The alloy has a thickness of at least 3 layers. Between 700 and 800 K, a second region of stability is observed with approximately 80–90% Pd. We speculated that this may correspond to a $CoPd_3$ alloy phase, but no LEED superstructure was detected nor was STM capable of resolving atomic scale information [20].

Experimental section

Two ultrahigh vacuum (UHV) systems were used in this study. The first chamber was an Omicron UHV system with a base pressure of 1×10^{-10} mbar which had facilities for RAIRS, low-energy electron diffraction (LEED), and scanning tunnelling microscopy (STM) experiments. LEED patterns were acquired using an Omicron SpectaLEED system. The sample was then transferred under UHV conditions to the STM chamber where images were acquired at room temperature in constant current mode using an electrochemically etched W tip. RAIRS measurements were carried out in UHV using a Nicolet Nexus 860 FTIR spectrometer fitted with a mercury cadmium telluride (MCT) detector cooled by liquid nitrogen, possessing a spectral range of 800–4000 cm^{-1}. The spectrometer was operated with a resolution of 4 cm^{-1}, at 256 scans per spectrum.

The second UHV system was located at the UK National MEIS facility at STFC Daresbury Laboratory [22]. 100 keV He^+ ions were utilised in this study. The ion beam had a well-defined energy (<0.1%) and low angular divergence (<0.1°). The end station consisted of a scattering chamber, a sample preparation and characterisation chamber, a sample transfer system, and a fast entry load lock. The preparation chamber was used for sample cleaning and characterisation (LEED/AES). In the scattering chamber, accurate beam alignment was achieved via a precision six-axis goniometer. A toroidal electrostatic energy analyser with position-sensitive detector measured the scattered ion intensities as functions of scattering angle and ion energy. The detector system produced two-dimensional intensity maps of the ion intensity over a 1.6% range of pass energy and a scattering angle range of 27° with a resolution of 0.3% and 0.3°, respectively. Full two-dimensional data sets were accumulated by joining together a series of 'tiles' which cover the required angle/energy range to produce a single scattered ion intensity map. Whilst two-dimensional data sets provided a complete picture of the scattering behaviour, it was normal to process the data by integrating over a range of angles or energies to produce one-dimensional plots. Plots of ion intensity versus scattering angle provide structural information that can be used to calculate parameters such as surface layer relaxation and to verify the alignment of the sample with respect to the beam. Energy spectra can be used to obtain quantitative compositional information. A detailed discussion of the MEIS technique can be found elsewhere [23].

In all experiments, the Pd{111} sample was cleaned by cycles of ion bombardment (Ar^+, 1.5 kV, sample 15 μA) and annealing to 1100 K until a sharp (1x1) LEED pattern characteristic of the Pd{111} surface was observed and no impurities were observed by AES. Co was deposited via metal vapour deposition at a rate of ~0.1 ML min^{-1} (1 ML is defined as 1.53×10^{15} atoms cm^{-2}, i.e. the atomic density of the Pd{111} surface). The growth of the Co (776 eV) Auger signal and the attenuation of the Pd feature at 330 eV were used to estimate the film thickness. The Co/Pd{111} surface was annealed to a pre-determined temperature and cooled to room temperature prior to MEIS and STM measurements. CO was dosed via a precision leak valve. CO gas was passed through a liquid nitrogen/acetone trap in order to remove any volatile metal carbonyls from the gas manifold. The absolute CO dose was calculated by multiplying the exposure time by the chamber pressure as measured by an ion gauge.

Results and discussion

Reflection absorption infrared spectroscopy

Fig. 1a shows the RAIR spectra taken during exposure of CoPd surfaces to 10^{-7} mbar CO at 300 K. Next to each trace are shown the pre-annealing temperature of the 4 ML Co/Pd{111} sample and the approximate surface composition (prior to CO exposure) derived from MEIS data reported in our earlier study [20]. Fig. 1b shows the RAIR spectra after evacuation of CO from the vacuum system. During exposure to 1000 L CO (10^{-7} mbar CO for 10000 s) at 300 K, two absorption bands are observed at 2015 and 2061 cm^{-1}. After evacuation of CO, these bands are still present in the RAIR spectra. In their study of CO adsorption on Co{0001}, Beitel et al. identified a CO adsorption band at ~2025 cm^{-1} under analogous dosing conditions [24]. This was assigned to the adsorption of CO in atop sites on Co surface atoms. In addition, Beitel et al. assigned a higher frequency feature (~2055 cm^{-1}) to the adsorption of CO at defects on a sputtered Co surface [24]. RAIRS indicates that the as-deposited Co film is continuous and relatively rough.

Annealing the 4 ML Co film to 450 K results in a flattening of the cobalt overlayer as evidenced by scanning tunnelling microscopy (STM); but no clear indication of surface alloy formation from MEIS data [20]. CO adsorption at 300 K on a 4 ML cobalt film on Pd{111} sample which has been annealed to 450 K results in a slight change in the frequencies and relative intensities of the two bands compared with the as-deposited Co/Pd{111} sample. The main feature is now observed at 2054 cm^{-1} with a shoulder at 2024 cm^{-1}. Upon removal of gas phase CO, a single relatively broad feature is observed at 2038 cm^{-1}. The bands in the 2000–2070 cm^{-1} range under these conditions of relatively low annealing temperatures are therefore assigned to CO on Co sites on the surface; the change in relative intensity being associated with the smoothing of the surface (i.e. decrease in the defect density) induced by the relatively gentle annealing procedure.

Annealing a 4 ML Co film on Pd{111} in the 500–600 K range corresponds to the onset of significant surface intermixing [20]. The RAIR spectra in the presence of 10^{-7} mbar CO are relatively similar for surfaces pre-annealed to 500 and 600 K with bands observed at 2013 cm^{-1} (500 K experiment) and 2006 cm^{-1} (600 K experiment). After evacuation of CO from the chamber, the peak intensities do not change noticeably, but a ~5 cm^{-1} red shift is observed in each case. A small positive band is also observed at approximately 1970 cm^{-1}, indicative of the loss or displacement of a CO species present as a background contaminant on the otherwise clean alloy surface. The absorption bands fall within the range expected for CO adsorbed on Co sites [25] under these conditions and there is no evidence for the presence of any Pd-related CO bands. When a low coverage of CO is adsorbed onto Co particles on alumina thin films, a band is observed at 1967 cm^{-1} [9]. The positive band at 1970 cm^{-1} is likely to correspond to the loss of the low coverage band (present following adsorption by CO from the background) and replacement by bands associated with a higher CO coverage.

Annealing to 650 K is at the upper limit of the temperature range of stability of the $Co_{50}Pd_{50}$ surface alloy which STM and LEED reveals has a p(2 × 1) structure consisting of alternating rows of Co and Pd atoms [20]. The surface atomic arrangement of this alloy is shown schematically in Fig. 2. Assuming that CO adsorbs either on Co sites or Pd sites, the only adsorption sites available would be atop or bridging sites. Exposure of the 650 K annealed sample to CO at 300 K results in a dramatic change to the RAIR spectra compared with the spectra from lower

Please cite this article as: A. Murdoch, et al., The influence of CO adsorption on the surface composition of cobalt/palladium alloys, Surf. Sci. (2015), http://dx.doi.org/10.1016/j.susc.2015.08.004

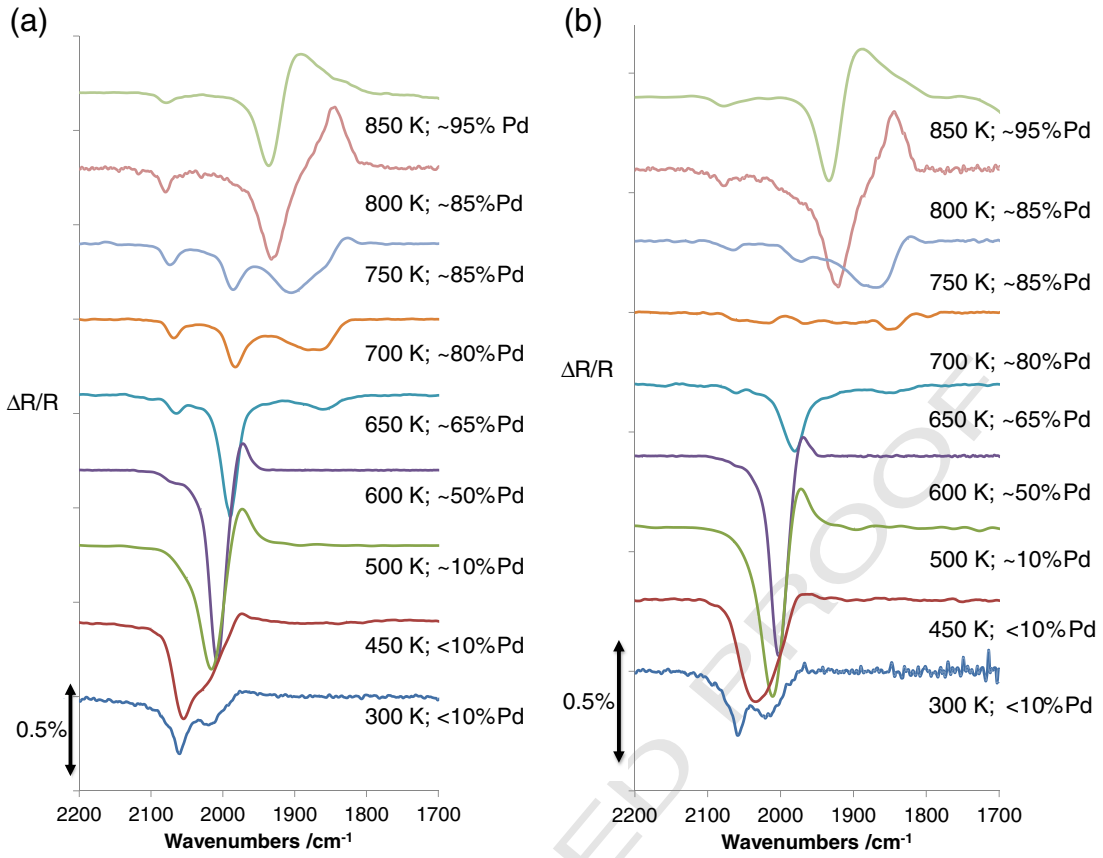

Fig. 1. a: RAIR spectra (measure during exposure to CO) as a function of annealing temperature for a 4 ML Co film on Pd{111} deposited at 300 K. Spectra were acquired during a 1000 L CO dose at 10^{-7} mbar CO with the sample held at 300 K. b: RAIR spectra as a function of annealing temperature for a 4 ML Co film on Pd{111} deposited at 300 K. Spectra were acquired after exposure to 1000 L CO at a pressure of 10^{-7} mbar with the sample held at 300 K.

pre-annealing temperatures. In the presence of 10^{-7} mbar CO, three bands are observed at 2067, 1988, and 1857 cm^{-1} with the 1988 cm^{-1} band being the dominant feature. After removal of the CO, the only clear feature remaining is at 1971 cm^{-1}. Following adsorption of CO onto Pd{111} at low coverage, a band is observed at 1850 cm^{-1} corresponding to adsorption in 3-fold hollow sites [26,27]. The band at 2067 cm^{-1} can be assigned to CO adsorbed in atop Pd sites [26,27]. Bridging CO on Pd{111} is observed at ~1940 cm^{-1} under analogous dosing conditions [26]. Hence it is most likely that the band at 1988 cm^{-1} may be assigned to atop CO on Co sites [9] though it should be noted that bridging CO on Pd(100) gives a band close to 1988 cm^{-1} [28,29].

The RAIR spectra following exposure to 10^{-7} mbar CO for 4 ML Co/Pd{111} samples annealed to 700 K and 750 K are similar to each other but significantly different to the spectrum following annealing to 650 K. STM and MEIS revealed that annealing in this temperature range induces significant further intermixing and a more Pd-rich alloy surface. The band at 1982 cm^{-1} is significantly less intense than the 1979 cm^{-1} band observed for the sample that had been annealed to 650 K. In addition, a more prominent broader band is observed at lower frequency. In the spectrum after pre-annealing to 750 K, this lower frequency band has a clear minimum at ~1920 cm^{-1}, whereas the 700 K sample shows an asymmetric peak covering a similar range but with a minimum at ~1870 cm^{-1}. The post-evacuation spectra of these annealing temperatures exhibits the loss of almost all intensity except in the lower frequency band of the sample pre-annealed to 750 K.

After annealing to 800 K, the CO RAIR spectra consist of a large band at 1929 cm^{-1} and a large positive band (indicating the loss of a CO species present in the background spectrum) at 1850 cm^{-1}. There is also a small band at 2074 cm^{-1}, corresponding to the small high-frequency peak in previous spectra. After evacuation of CO, the peak intensities remain essentially constant and shift down by <5 cm^{-1}. The RAIR spectra of the sample pre-annealed to 850 K is similar to that following the 800 K annealing treatment, except that the positive band is shifted to above 1900 cm^{-1}. In this annealing region, MEIS/STM reveals surfaces containing ~80% Pd and exhibiting relatively long range moiré structures.

The small high-frequency peak partially decreases in intensity from the 800 K annealed surface to the 850 K annealed surface and the large positive peak shifts down and broadens. Post-evacuation spectra indicate similar behaviour to the 800 K annealed surface: The peak intensity does not appear to change and there is a very small shift down in frequency of the main peak. The RAIR spectra acquired for the samples

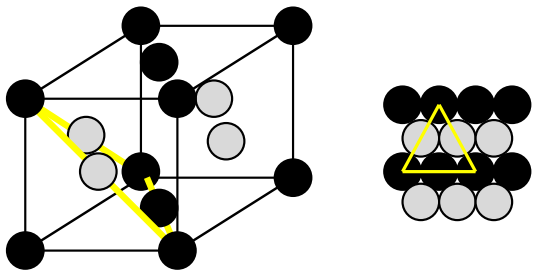

Fig. 2. Schematic diagram showing the bulk and {111} surface termination of the ordered CoPd alloy [20].

Please cite this article as: A. Murdoch, et al., The influence of CO adsorption on the surface composition of cobalt/palladium alloys, Surf. Sci. (2015), http://dx.doi.org/10.1016/j.susc.2015.08.004

annealed to 800 K and above are very similar to those reported by Kuhn and Goodman for CO adsorption on Pd{111} at 10^{-7} mbar and 300 K [26].

Medium energy ion scattering

In order to acquire MEIS data, the sample was aligned along the <1 1 2> azimuthal direction utilising the [1 1 4] incident geometry (Fig. 3) for the ion beam. For the clean Pd{111} surface, this corresponds to a geometry whereby each of the top 3 layers of the surface are illuminated while each subsequent layer lies, to a good approximation, within the shadow cones associated with the incident ion beam. Intensity versus scattering angle data were acquired over a scattering angle range from 75° to 115°. For the ideal Pd{111} surface, the outgoing [1 1 0] direction is a well-defined blocking channel at a scattering angle of 109.5°. At this angular position, the ions reaching the detector almost exclusively result from collisions with atoms in the outermost surface layer. When Co is deposited onto Pd{111}, the substantial lattice mismatch (2.50 Å (Co) v 2.75 Å (Pd)) results in non-pseudomorphic growth. The double alignment geometry associated with the 1-layer geometry for Pd{111} is ineffective at shadowing and blocking the Co overlayer so the total yield of scattered ions is substantially increased. The scattered ion yield as a function of annealing temperature is shown in Fig. 4a for the 1-layer [1 1 0] geometry and in Fig. 4b for the 2-layer [3 −3 2] geometry. The intensity of each elemental peak has been normalised to allow a comparison of the relative visibilities of each element by taking into account the Rutherford cross section, i.e. by dividing by the square of the atomic number [23]. After annealing to 850 K, the total visibility of Co and Pd reaches a minimum value corresponding to that observed for the Pd{111} clean surface. The as-deposited Co film displays a much higher visibility consistent with the fact that the overlayer does not grow pseudomorphically on the Pd{111} substrate. As the sample is annealed, the total visibility drops smoothly to the value of the clean surface. It should be noted that the total visibility of Pd remains relatively constant regardless of the annealing treatment. As can be seen in Fig. 5, the Pd intensity is made up of a subsurface contribution and a surface contribution. When there is a thick Co film, all of the Pd intensity comes from the subsurface feature—i.e. Pd atoms that are ineffectively shadowed by the non-pseusomorphic overlayer.

The RAIRS data for CO adsorption on the 4 ML Co/Pd{111} surface annealed in the 500–600 K range are consistent with a surface

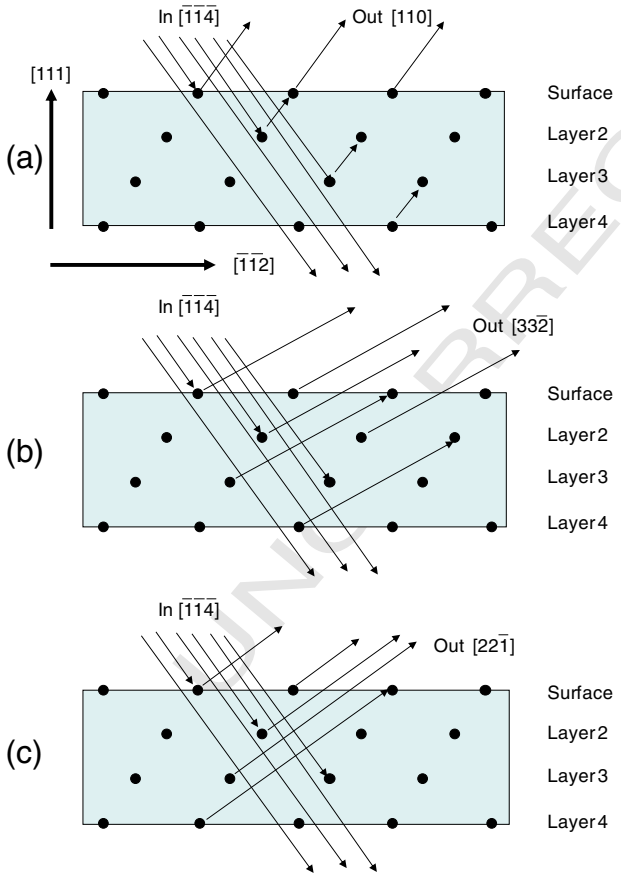

Fig. 3. Schematic diagrams showing the ion beam trajectories utilised to achieve (a) 1-, (b) 2-, and (c) 3-layer geometries in the azimuth of the fcc {111} surface. The arrows represent ion trajectories and show, for example, how the 1st, 2nd, and 3rd layer atoms are visible to the incident beam while, by contrast, the 4th layer atoms are shadowed. Similarly, outgoing trajectories show how the phenomenon of blocking can be utilised to achieve layer specific information.

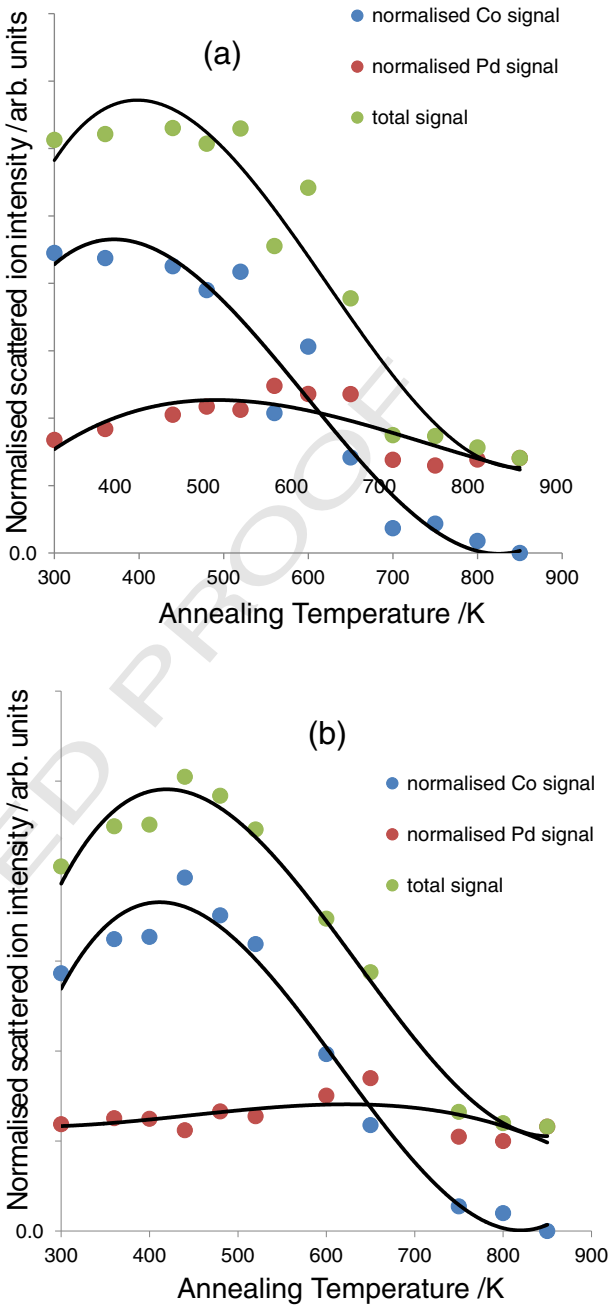

Fig. 4. Scattered ion intensity in the (a) 1-layer and (b) 2-layer geometry of the clean Pd{111} surface. The intensity of the Co and Pd peaks were measured separately and then normalised to take into account the dependence of the scattering cross section on the square of the atomic number.

Please cite this article as: A. Murdoch, et al., The influence of CO adsorption on the surface composition of cobalt/palladium alloys, Surf. Sci. (2015), http://dx.doi.org/10.1016/j.susc.2015.08.004

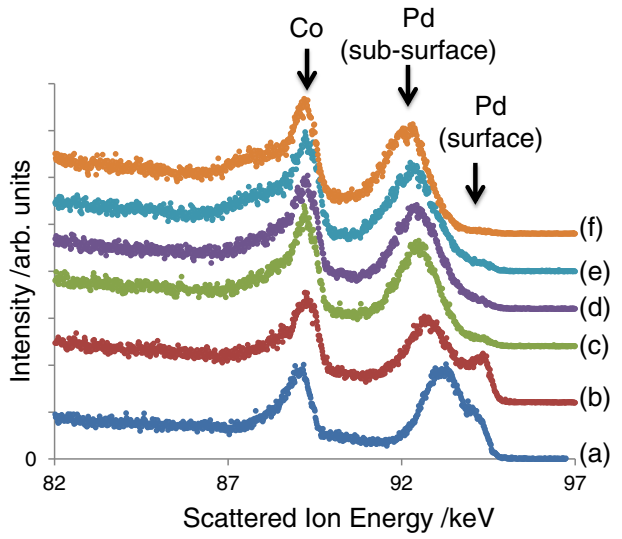

Fig. 5. Scattered ion intensity as a function of ion energy in the 2-layer geometry of clean Pd{111} for a 6 ML Co film on Pd{111} (a) as deposited at 300 K; (b) annealed to 560 K; (c) after exposure to 1000 L at 10^{-7} mbar CO; (d) after exposure to 1000 L at 10^{-6} mbar CO;(e) after exposure to 1000 L at 10^{-5} mbar CO;(f) after exposure to 1000 L at 10^{-4} mbar CO. All CO exposures were carried out at 300 K.

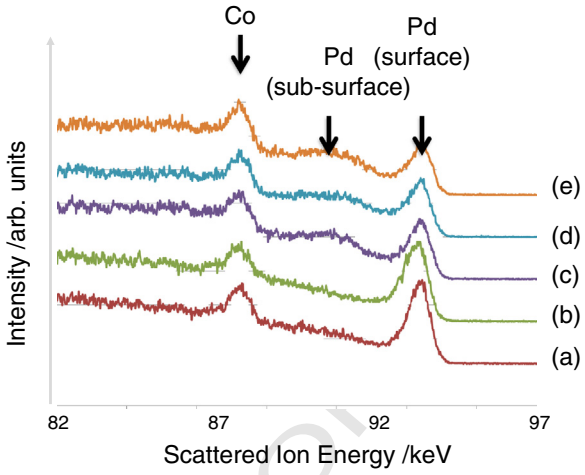

Fig. 6. Scattered ion intensity as a function of ion energy in the 2-layer geometry of clean Pd{111} for a 6 ML Co film on Pd{111} (a) annealed to 700 K; (b) after exposure to 1000 L at 10^{-7} mbar CO; (c) after exposure to 1000 L at 10^{-6} mbar CO;(d) after exposure to 1000 L at 10^{-5} mbar CO;(e) after exposure to 1000 L at 10^{-4} mbar CO. All CO exposures were carried out at 300 K.

containing exclusively Co atoms despite the fact that MEIS data show a significant surface Pd content. A MEIS experiment was carried out by depositing a 6 ML Co film onto Pd{111} at 300 K. The MEIS intensity versus energy spectrum is shown in Fig. 5a. On annealing to 560 K, a surface Pd peak is observed at 94.1 keV (Fig. 5b). Additional peaks are observed at 89.2 keV (Co) and a broader feature at 92.8 keV which is associated with ions scattered from subsurface Pd atoms. These atoms are visible in this double alignment geometry since they are covered by (pre-dominantly) Co atoms with a contracted lattice compared to Pd{111}. The energy offset is caused by the inelastic energy loss associated with ions travelling through several layers of the metallic surface [23].

Exposing this surface to 1000 L Co at 10^{-7} mbar and 300 K results in the spectrum shown in Fig. 5c. It is readily apparent that the surface Pd peak has completely disappeared consistent with adsorbate-induced segregation of Co to the surface by CO adsorption. It should be noted that no time-dependent changes were observed in the RAIR spectra during the CO dose. This suggests that any compositional changes are rapid compared to the timescale of acquisition of the RAIR spectra. The spectra are subsequently unchanged by exposure to 1000 L CO at 10^{-6}, 10^{-5}, and 10^{-4} mbar (Figs. 5d–f). Prior to CO exposure, the small surface Pd peak corresponds to <20% of a monolayer. Assuming that surface mixing results in Pd atoms randomly distributed in a Co matrix, most Pd atoms will be present as isolated atoms and few Pd clusters will be found. Exposure of this surface to 10^{-7} mbar CO results in the complete disappearance of the surface Pd peak consistent with adsorbate-induced segregation of Co to the surface. It is likely that the driving force for this segregation is the fact that CO adsorption on isolated Pd atoms corresponds to ~0.7 eV [15] while adsorption on Co sites is significantly stronger (1.2 eV) [30].

A second MEIS experiment was undertaken by depositing a 6 ML Co film and annealing to 700 K. Auger electron spectroscopy and MEIS confirm that the near-surface region has an approximate composition of $Co_{50}Pd_{50}$, but MEIS indicates that the surface layer is slightly Pd rich (~70% Pd). As shown in Fig. 6, exposure of this surface to CO results in a slight decrease in the intensity of the surface Pd peak and an increase in the visibility of subsurface Pd. These two observations are self-consistent; the increase in the subsurface signal is associated with the surface layer becoming less Pd-like in terms of its lattice structure as was shown in Figs. 4a and b. The intensity of the surface Pd peak in the MEIS spectra shown in Fig. 6 reveals that the surface composition tends towards $Pd_{50}Co_{50}$ which is the coverage at which the clean surface displays a $p(2 \times 1)$ structure consisting of alternating rows of Pd and Co atoms. The RAIRS data indicate that three-fold Pd sites are present which would not be the case if the ordered alloy structure (Fig. 2) were adopted. Rupprechter et al recently reported that exposure of a similar PdZn{111} surface to CO results in a redistribution of surface atoms within the surface layer to minimise the overall energy. [19] It is possible that CO has a similar effect on the PdCo surface such that while, under vacuum conditions, the $p(2 \times 1)$ PdCo structure is favoured, after exposure to CO, the surface reconstructs in order to maximise the favoured Pd_3 and Co_1 sites at the surface.

In the presence of CO, cobalt-rich Co/Pd alloys tend towards surfaces containing pure cobalt. CO induces segregation of cobalt to surfaces that are initially enriched in Pd but with a significant reservoir of cobalt in the near-surface region. At higher annealing temperatures, RAIRS indicates that CO adsorption tends towards the behaviour expected for Pd(111). Under these conditions, the amount of cobalt in the near-surface region has fallen to a few atomic percent (Figs. 4a–b) as significant dissolution of cobalt into the bulk has occurred [20]. At room temperature, adsorbate-induced segregation is likely to be kinetically limited to atoms in the top few layers, so any segregation would have a minor effect on the surface composition. In catalytic terms, it would be interesting to investigate how CO/H_2 mixtures influence the surface composition of the PdCo surface.

In cases such as this where the adsorption of CO on the two pure elements gives quite different vibrational spectra, the combination of MEIS and surface vibrational spectroscopy is a powerful probe of surface composition. MEIS is ideally suited for this type of investigation as it is capable of probing surface composition with close to monolayer resolution and it is relatively insensitive to the presence of light molecular adsorbates. This contrasts with XPS where the molecular adsorbate attenuates the signal from the metal surface and complicates the analysis in terms of identifying segregation effects.

Conclusions

The vibrational spectra of CO adsorbed on CoPd alloys on Pd{111} varies strongly with initial Pd content. At annealing temperatures up to 600 K, CO adsorption onto a 4 ML Co/Pd{111} surface displays evidence for adsorption exclusively on Co sites despite the fact that MEIS indicates that the surface has significant Pd content prior to adsorption of CO.

Please cite this article as: A. Murdoch, et al., The influence of CO adsorption on the surface composition of cobalt/palladium alloys, Surf. Sci. (2015), http://dx.doi.org/10.1016/j.susc.2015.08.004

MEIS shows that when surface alloys are created with <20% Pd, the adsorption of CO causes segregation of Co to the surface and the loss of any detectable Pd in the surface layer. This effect can be explained by the fact that at this starting concentration, most Pd atoms are present in isolation on the surface. Adsorption of CO in atop Co sites is energetically much more favourable than adsorption on atop Pd sites.

When a surface is created which is slightly Pd enriched, MEIS shows that the surface restructures in the presence of CO to produce an approximately 50:50 CoPd composition. However, the RAIR spectra indicate the significant presence of three-fold Pd sites at the surface. Such sites are not present on the p(2 × 1) CoPd alloy which exists under UHV conditions in the absence of CO, suggesting that the adsorption of CO causes a lateral rearrangement of the 50:50 alloy to allow local clustering of Pd atoms to produce Pd_3 sites which adsorb CO strongly.

Uncited reference

[21]

Acknowledgements

AM is grateful for funding from SASOL Technology UK Ltd (PhD studentship); JG is grateful for the award of a fellowship from the Knut and Alice Wallenberg Foundation. TEJ and AGT acknowledge EPSRC funding of postdoctoral research (EP/E047580/1). The MEIS facility was funded via EPSRC grant EP/E003370/1. We are grateful for access to the STM chamber of Professor NV Richardson.

References

[1] F. Fischer, H. Tropsch, Brennst.-Chem. 7 (1926) 97.
[2] E. de Smit, B.M. Weckhuysen, Chem. Soc. Rev. 37 (2008) 2758.
[3] F. Diehl, A.Y. Khodakov, Oil Gas Sci. Technol. Rev. Inst. Fr. Pet. 64 (2009) 11.
[4] A.Y. Khodakov, Catal. Today 144 (2009) 251.
[5] L. Guczi, L. Borko, Catal. Today 64 (2001) 91.
[6] L. Guczi, L. Borko, Z. Schay, D. Bazin, F. Mizukami, Catal. Today 65 (2001) 51.
[7] D.Y. Xu, W.Z. Li, H.M. Duan, Q.J. Ge, H.Y. Xu, Catal. Lett. 102 (2005) 229.
[8] A.F. Carlsson, M. Naschitzki, M. Baumer, H.J. Freund, Surf. Sci. 545 (2003) 143.
[9] A.F. Carlsson, M. Baumer, T. Risse, H.J. Freund, J. Chem. Phys. 119 (2003) 10885.
[10] A.F. Carlsson, M. Naschitzki, M. Baumer, H.J. Freund, J. Phys. Chem. B 107 (2003) 778.
[11] M. Heemeier, A.F. Carlsson, M. Naschitzki, M. Schmal, M. Baumer, H.J. Freund, Angew. Chem. Int. Ed. 41 (2002) 4073.
[12] V.R. Calderone, N.R. Shiju, D.C. Ferre, G. Rothenberg, Green Chem. 13 (2011) 1950.
[13] V. Ponec, Appl. Catal. A Gen. 222 (2001) 31.
[14] W. Yu, M.D. Porosoff, J.G. Chen, Chem. Rev. 112 (2012) 5780.
[15] P. Liu, J.K. Norskov, Phys. Chem. Chem. Phys. 3 (2001) 3814.
[16] S. Kezilebieke, A. Amokrane, M. Boero, S. Clair, M. Abel, J.-P. Bucher, Nano Res. 7 (2014) 888.
[17] S. Zafeiratos, S. Piccinin, D. Teschner, Catal. Sci. Technol. 2 (2012) 1787.
[18] K.J. Andersson, F. Calle-Vallejo, J. Rossmeisl, L. Chorkendorff, J. Am. Chem. Soc. 131 (2009) 2404.
[19] C. Weilach, S.M. Kozlov, H.H. Holzapfel, K. Foettinger, K.M. Neyman, G. Rupprechter, J. Phys. Chem. C 116 (2012) 18768.
[20] A. Murdoch, A.G. Trant, J. Gustafson, T.E. Jones, T.C.Q. Noakes, P. Bailey, C.J. Baddeley, Surf. Sci. 608 (2013) 212.
[21] I. Horcas, R. Fernandez, J.M. Gomez-Rodriguez, J. Colchero, J. Gomez-Herrero, A.M. Baro, Rev. Sci. Instrum. 78 (2007) 013705.
[22] P. Bailey, T.C.Q. Noakes, D.P. Woodruff, Surf. Sci. 426 (1999) 358.
[23] R.M. Tromp, Practical Surface Analysis, in: D. Briggs, M.P. Seah (Eds.), Ion and Neutron Spectroscopy, 2nd ed., vol. 2, John Wiley and Sons Ltd, 1992.
[24] G.A. Beitel, A. Laskov, H. Oosterbeek, E.W. Kuipers, J. Phys. Chem. 100 (1996) 12494.
[25] R.L. Toomes, D.A. King, Surf. Sci. 349 (1996) 1.
[26] W.K. Kuhn, J. Szanyi, D.W. Goodman, Surf. Sci. 274 (1992) L611.
[27] A.M. Bradshaw, F.M. Hoffmann, Surf. Sci. 72 (1978) 513.
[28] M. Frank, M. Baumer, Phys. Chem. Chem. Phys. 2 (2000) 3723.
[29] K. Wolter, O. Seiferth, H. Kuhlenbeck, M. Baumer, H.J. Freund, Surf. Sci. 399 (1998) 190.
[30] J. Lahtinen, J. Vaari, K. Kauraala, E.A. Soares, M.A. Van Hove, Surf. Sci. 448 (2000) 269.

Please cite this article as: A. Murdoch, et al., The influence of CO adsorption on the surface composition of cobalt/palladium alloys, Surf. Sci. (2015), http://dx.doi.org/10.1016/j.susc.2015.08.004